Use of polarized optical absorption to obtain structural information for Na^+/Nd^{3+} β''-alumina

Sverker Edvardsson
Department of Physics and Mathematics, Mid Sweden University, S-851 70 Sundsvall, Sweden

Mattias Klintenberg and John O. Thomas
Institute of Chemistry, Uppsala University, Box 531, S-751 21 Uppsala, Sweden

(Received 1 May 1996)

Part of the optical absorption spectrum is calculated for the Nd^{3+}-doped Na^+ β''-alumina using a molecular-dynamics- (MD) based approach. The Judd/Ofelt (J/O) theory is modified (and several approximations removed) to treat polarized transition intensities for rare-earth ions in a solid host. Stark-level energies and eigenfunctions of the ground state ($^4I_{9/2}$) and excited multiplets ($^4F_{3/2}$,$^2P_{1/2}$) are also calculated for the local environments involved. Energies and polarized transition intensities between individual Stark levels are thus calculated simultaneously for several hundreds of MD-generated environments; summation gives the total bandshape. A high proportion of Beevers-Ross-site occupation (>50%) is indicated for low Nd^{3+} concentrations in β''-alumina. The contrary is observed experimentally for high Nd^{3+} concentrations, i.e., then midoxygen site occupation dominates. It is demonstrated that ions in different local environments contribute differently to the absorption spectrum and, particularly, how the polarization of the various transitions changes for ions occupying different sites. Temperature dependence aspects are also considered. [S0163-1829(96)09047-9]

INTRODUCTION

The Judd/Ofelt (J/O) theory and many other theoretical investigations have earlier been used to predict spectral intensities and energies for rare-earth (RE) ions in optical materials.[1–9] In optically anisotropic media, J/O theory must be modified to include the polarization of the incoming light, the orientations of the RE ions, and thus the symmetry of the Stark states for the various environments. Stark states are usually predicted by group theory, where it is assumed that the RE ion is situated in a perfectly symmetric environment. It is then possible to predict the number of Stark levels split in this particular symmetry. No information regarding the quantitative Stark-level energies can be obtained, however. If actual numbers are desired, it is necessary to diagonalize the energy matrix. Group theory can also be used qualitatively to derive nonvanishing crystal-field parameters (CFP's). Although this approach works well for crystals, it is clear that it must be modified for complex disordered materials. In a previous paper,[10] we have presented a method for calculating the intensities according to Judd/Ofelt theory, where the positions of the ions surrounding the optical ion, needed to calculate the odd-order crystal-field parameters, were generated using molecular-dynamics (MD) simulation. The corresponding calculation of energies is presented here, along with a method for the treatment of polarization. The polarized intensities and energies are calculated simultaneously for a given environment. The basic assumption is that MD produces a sequence of physically acceptable environments around each RE ion in the simulation box. These are used to calculate a number of energies and intensities. A summation is then performed to give the total absorption band. This can be compared with the experimental situation, where a huge number of environments occur in the sample. This approach can prove particularly useful for nonstoichiometric or amorphous systems, where local structure is not readily accessible, e.g., liquids, glasses, polymers, etc. The method has earlier been applied to the case of Nd^{3+} ions in the partially ordered β''-alumina host framework. Experimental σ-polarized intensities were reproduced reasonably well for the solid Na^+/Nd^{3+} β''-alumina system.[11] However, the π-polarized intensities were exaggerated, since the slightly modified polarized J/O theory presented in Ref. 12 does not include the eigenfunctions of the Stark levels, i.e., RE-ion orientation is lost. For the structural situation in β''-alumina (see below), σ-polarization corresponds to light polarized along the conduction planes, and π polarization corresponds to light polarized along the c axis. It is well known that the sodium ions are extremely mobile within the conduction planes. The dynamical fluctuations sensed by a RE ion in the c direction are much smaller. The crystal-field perturbations in the ab directions are therefore much stronger, thus causing the σ oscillator strengths to be greater than the π. This can also be seen in a experiment by Dai *et al.*[13] where $\Omega_{2\sigma}=39.6$ and $\Omega_{2\pi}=10.7$. The lost RE-ion orientation in the theory of Alfrey *et al.*[12] would imply roughly the same values for both polarizations, i.e., $\Omega_{2\pi}\sim\Omega_{2\sigma}$. This is indeed observed in Table IV of Ref. 11. It can thus be concluded that their ''polarized'' J/O approach must be modified. The various Stark levels should be included and described by their appropriate eigenfunctions. The symmetries of these separate Stark levels are different, so the polarized transitions between different Stark levels in the ground state to an excited state will also be different. In this paper, we therefore extend the approach of Refs. 10 and 11 to include the calculation of energy levels involving even-order CFP's. This has normally been done by fitting experimentally obtained energies to a model Hamiltonian,[14] or by using *ab initio* methods to calculate CFP's for ions in a particular symmetry.[15] An approach similar to that presented here has earlier been used by Weber and Brawer[16] to calculate energy-level splittings in RE-doped fluoroberyllate glasses using structural configurations obtained from Monte Carlo and MD simulations.

THEORY

Perturbation potential

If the crystal fields experienced by the $4f$ electrons are sufficiently weak, the effect of the environment can be treated as a first-order perturbation. The contribution to the Hamiltonian from the external crystal fields may be written:

$$H_{\mathrm{CF}}=-\sum_i \sum_{t=0}^{\infty} \sqrt{\frac{4\pi}{2t+1}} \sum_{p=-t}^{t} A_{t,p} r_i^t Y_{t,p}(\theta_i,\phi_i).$$

The crystal-field parameters for an ionic point-charge model with shielding[8] included are given by

$$A_{t,p}=(1-\sigma_t)(-1)^p \sqrt{\frac{4\pi}{2t+1}} \sum_j q_j e R_j^{-t-1} Y_{t,-p}(\Theta_j,\Phi_j), \tag{1}$$

where the sum runs over all neighboring charges q $(=ge)$ located at (R,Θ,Φ). The even CFP's determine the Stark energies, whereas the odd CFP's are related to the intensities. Experiment often reveals that some refinement of crystal-field theory is necessary. If polarization (α) of nearest-neighbor ions cannot be neglected, one can take approximate account of this by replacing the factor $q_j e R_j^{-t-1}$ in Eq. (1) by $q_j e R_j^{-t-1}+\mu_j e(t+1) R_j^{-t-2}+\frac{1}{2} Q_j e(t+1)(t+2) R_j^{-t-3}$, where $\mu_j=\alpha_j E$ is the component of the dipole moment directed towards the RE nucleus, and Q_j is the component of the quadrupole moment. More refined crystal-field models have been made by, for example, Newman.[17] Shielding-antishielding is another effect frequently taken into account; it arises when the crystal field polarizes the outer electrons (primarily in $5s^2 5p^6$) in such a way that the $4f$ electrons experience a different crystal field. The shielding parameters (σ_t) was calculated for Nd^{3+} by Sengupta *et al.*[8] (see also Refs. 7 and 9). In many close-packed crystalline compounds, it is not a good approximation to neglect covalent charge distributions or polarization effects. However, it is believed that a point-charge model can be successful in providing the magnitudes of the higher order A_{tp}'s in most ionic crystals, if it is recognized that Hartree-Fock radial wave functions do not give an adequate approximation to the true radial charge distribution.[18] It should be noted that the transition intensities studied in the current work depend only on higher-order A_{tp}'s $(t=3,5,7)$; our radial wave functions are based on the more realistic Hartree-Fock-Slater-Dirac method, and shielding is included. It is further believed that the special structural nature of β''-alumina justifies the use of a point-charge model, since (i) β''-alumina is a highly ionic compound (cf. diffraction and spectroscopic studies[19–22]), and (ii) the nearest-neighbor Nd-O distances within the conduction planes are up to 25% longer than, for example, in Nd_2O_3 (2.3→2.8 Å), making polarization effects much smaller. Our main purpose is here to study how the diffusing Na^+ ions affect the Nd^{3+} ions (in the open liquidlike conduction planes) and also how the absorption spectrum is influenced by the various Nd^{3+} sites.

Energy matrix

The expressions needed for calculating the Stark energies and their eigenfunctions are given here. Another popular approach is to use ''operator equivalents;'' see, for example, Stevens.[23] The crystal-field Hamiltonian above can be incorporated into degenerate perturbation theory. In Russel-Saunders coupling, the free-ion wave functions for the RE ions can be characterized by $|\gamma SLJM_J\rangle$. These states can be expanded as a linear combination of determinantal product states[24] by first transforming to SLM_SM_L quantization, i.e.,

$$|\gamma SLJM_J\rangle=\sum_{M_S M_L} C(M_S,M_L)|\gamma SLM_S M_L\rangle,$$

where $C(M_S,M_L)$ are the usual Clebsch-Gordan coefficients and the determinantal product states are given by

$$|\gamma SLM_S M_L\rangle=\sum_k c_k\{K_1^{(k)}K_2^{(k)}\cdots K_N^{(k)}\},$$

where c_k are normalizing constants and $\{K_1K_2\cdots K_N\}$ is a general determinantal product state with $K_i=(n_i l_i m_{s_i} m_{l_i})$. In the case of Nd^{3+}, the $4f^3$ configuration implies that $N=3$. Notice that H_{CF} is spin independent and, since it is a sum of single-particle operators h_{CF}, the elements in the perturbation matrix can now be calculated according to (see Refs. 24 and 25):

$$\langle\gamma SLJM_J|H_{\mathrm{CF}}|\gamma SLJM_J'\rangle=\sum_{m_l,m_l'} c_{m_l m_l'}\langle nlm_l|h_{\mathrm{CF}}|nlm_l'\rangle. \tag{2}$$

The material-independent $c_{m_l m_l'}$ constants could be calculated by first determining the constants c_k above using shift operators, and then performing direct integration as outlined in Ref. 24. This is extremely tedious, however. Instead, the $c_{m_l m_l'}$ constants are calculated using fractional parentage coefficients (see Racah[26]) through the following expression:

$$\begin{aligned} c_{m_l m_l'}=&\sum_{M_S M_L M_L'}\langle\gamma SLJM_J|\gamma SLM_S M_L\rangle \\ &\times\langle\gamma SLM_S M_L'|\gamma SLJM_J'\rangle \\ &\times\sum_{\gamma_1 S_1 L_1}(G^{\gamma SL}_{\gamma_1 S_1 L_1})^2\sum_{M_{L_1}}\langle L_1 lLM_L'|L_1 lM_{L_1}' m_l'\rangle \\ &\times\langle L_1 lM_{L_1} m_l|L_1 lLM_L\rangle, \end{aligned}$$

where $G^{\gamma SL}_{\gamma_1 S_1 L_1}$ are the fractional parentage coefficients. The single-particle matrix element is given by

$$\begin{aligned}\langle nlm_l|h_{\mathrm{CF}}|nlm_l'\rangle=&-\sum_{t=2,4,6}\sum_{p=-t}^{t} A_{t,p}\langle r^t\rangle(-1)^{m_l}(2l+1) \\ &\times\begin{pmatrix} l & t & l \\ 0 & 0 & 0\end{pmatrix}\begin{pmatrix} l & t & l \\ -m_l & p & m_t'\end{pmatrix}, \end{aligned} \tag{3}$$

where the radial part is $\langle r^t\rangle=\int_0^\infty r^2 R_{nl}^* r^t R_{nl} dr$.

Solving the secular equation for the $(2J+1)\times(2J+1)$ Hermitian matrix $(\langle\gamma SLJM_J|H_{\mathrm{CF}}|\gamma SLJM_J'\rangle)$ results, for half-integer J values (odd number of electrons), in $2J+1$

eigenfunctions but only $J+1/2$ eigenvalues, since the wave functions are interrelated through Kramer's theorem.[27] Each doubly degenerate Stark level is described by two eigenfunctions. Only about one-fourth $[(J+1)^2-1/4]$ of the elements need to be considered, because there are obvious relations [see Eq. (2)] connecting the matrix element $\langle M_J|H_{\rm CF}|M_J'\rangle$ to $\langle M_J'|H_{\rm CF}|M_J\rangle$, $\langle -M_J|H_{\rm CF}|-M_J'\rangle$, and $\langle -M_J'|H_{\rm CF}|-M_J\rangle$ (SLJ implicit).

Oscillator strengths

Calculation of optical absorption intensities for lanthanide ions has usually been made using Judd-Ofelt theory.[1,2] Here, the odd terms in the crystal-field expansion are responsible for the mixing of odd-parity excited configurations $(4f^{N-1}n'l')$ into the $4f^N$ states, thereby making otherwise parity-forbidden electric-dipole transitions allowed. An attempt to include polarization dependence for the oscillator strengths was made by Alfrey *et al.*:[12]

$$P_q=\chi\,\frac{8\pi^2 m\nu}{(2J+1)h}\times\sum_{\lambda=2,4,6}\Omega_{\lambda,q}|\langle 4f^N[S,L]J\|U^{(\lambda)}\|4f^N[S',L']J'\rangle|^2. \tag{4}$$

$\chi=(n^2+2)^2/9n$ is the Lorentz local field correction for the refractivity of the medium; q takes account of polarization of the incoming light; m is the mass of an electron; ν is the frequency of the transition band; h is Planck's constant; $\langle i\|U^{(\lambda)}\|f\rangle$ are the doubly reduced transition matrix elements of the spherical tensor operators; $(2J+1)^{-1}$ is an assumed degeneracy of the ground state, and $\Omega_{\lambda,q}$ are the polarized J/O intensity parameters, which include the CFP's. Unfortunately, this slightly modified ''polarized'' J/O theory does not include the Stark-level energies; nor are the eigenfunctions of the Stark levels included, i.e., there is no ion orientation with respect to the incoming radiation field. We are now in a position to correct Eq. (4) and, at the same time, remove some of the approximations in standard Judd-Ofelt theory. Starting with the electric dipole transition element between two states $|i\rangle$ and $|f\rangle$ [Eq. (13) in the classic paper by Judd[1]]:

$$\langle i|D_q^{(1)}|f\rangle=\sum_{\lambda tp}(2\lambda+1)(-1)^{p+q}A_{tp}\begin{pmatrix}1&\lambda&t\\ q&-p-q&p\end{pmatrix}\times\left\langle\sum_M a_M\Psi_{JM}|U^{\lambda}_{p+q}|\sum_{M'}a_{M'}\Psi_{J'M'}\right\rangle\Xi(t,\lambda). \tag{5}$$

Using the Wigner-Eckart theorem, we can write

$$\left\langle\sum_M a_M\Psi_{JM}|U^{\lambda}_{p+q}|\sum_{M'}a_{M'}\Psi_{J'M'}\right\rangle=\sum_{MM'}a_M^*a_{M'}\langle\Psi_{JM}|U^{\lambda}_{p+q}|\Psi_{J'M'}\rangle=\sum_{MM'}a_M^*a_{M'}(-1)^{J-M}\begin{pmatrix}J&\lambda&J'\\ -M&p+q&M'\end{pmatrix}\times\langle\Psi_J\|U^{\lambda}\|\Psi_{J'}\rangle.$$

The transition element thus becomes

$$\langle i|D_q^{(1)}|f\rangle=\sum_{\lambda tpMM'}(2\lambda+1)(-1)^{p+q}A_{tp}\times\begin{pmatrix}1&\lambda&t\\ q&-p-q&p\end{pmatrix}a_M^*a_{M'}(-1)^{J-M}\times\begin{pmatrix}J&\lambda&J'\\ -M&p+q&M'\end{pmatrix}\langle\Psi_J\|U^{\lambda}\|\Psi_{J'}\rangle\Xi(t,\lambda), \tag{6}$$

where $\Xi(t,\lambda)$ is listed in Ref. 1. All relevant parameters (radial integrals, energy denominators, etc.) included in $\Xi(t,\lambda)$ are listed in Table I. Kramer's theorem tells us that the Stark levels are doubly degenerated, so both the initial and final state are degenerate. The two wave functions of the lower state ($i=1,2$) are written

$$\alpha_i=\sum_M a_{iM}\Psi_{JM}$$

and the two wave functions of the upper state ($j=1,2$) are

$$\beta_j=\sum_{M'}a_{jM'}\Psi_{J'M'},$$

where the wave functions α_i and β_j are simply the eigenfunctions from the energy matrix above and the Stark ener-

TABLE I. Radial integrals, energy denominators and reduced matrix elements for Nd^{3+} (from Ref. 11) in atomic units.

$\langle 4f\|r^2\|4f\rangle$	1.22
$\langle 4f\|r^4\|4f\rangle$	3.87
$\langle 4f\|r^6\|4f\rangle$	26.1
$\langle 4f\|r^8\|4f\rangle$	307
$\langle 4f\|r\|5d\rangle$	0.83
$\langle 4f\|r^3\|5d\rangle$	4.45
$\langle 4f\|r^5\|5d\rangle$	37.3
$\Delta E(5d)$	0.32[a]
$\Delta E(n'g)$	1.13[a]
$\langle {}^4I_{9/2}\|\|U^2\|\|{}^2P_{1/2}\rangle$	0
$\langle {}^4I_{9/2}\|\|U^4\|\|{}^2P_{1/2}\rangle$	−0.1884
$\langle {}^4I_{9/2}\|\|U^6\|\|{}^2P_{1/2}\rangle$	0
$\langle {}^4I_{9/2}\|\|U^2\|\|{}^4F_{3/2}\rangle$	0
$\langle {}^4I_{9/2}\|\|U^4\|\|{}^4F_{3/2}\rangle$	0.4778
$\langle {}^4I_{9/2}\|\|U^6\|\|{}^4F_{3/2}\rangle$	0.2317

[a]Reference 40.

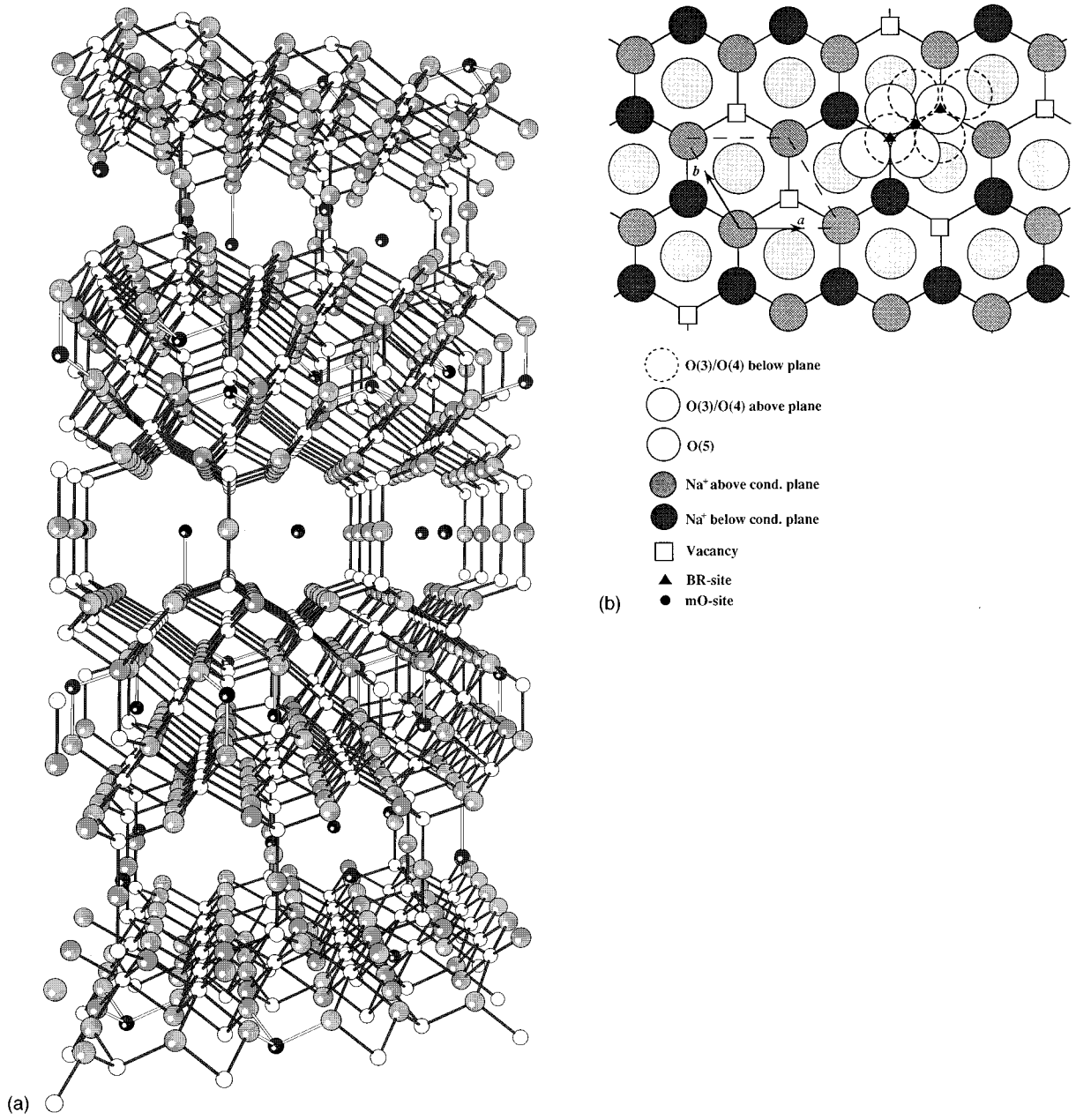

FIG. 1. (a) The spinel blocks. The Nd^{3+} ions are exchanged into the conduction planes between the rigid spinel blocks. (b) Schematic drawing of the conduction plane of β''-alumina showing the local environment of the MO and BR sites (unit-cell dashed).

gies E_α and E_β are their eigenvalues. The oscillator strength between two individual Stark levels α and β becomes

$$P_q(\alpha,\beta)=\frac{1}{2}\,\chi\,\frac{8\pi^2 m\nu_{\alpha\beta}}{h}\left(\sum_{i=1,2}\sum_{j=1,2}|\langle\alpha_i|D_q^{(1)}|\beta_j\rangle|^2\right)\times\frac{\exp(-E_\alpha/k_bT)}{\sum_{\alpha=1}^{J+1/2}\exp(-E_\alpha/k_bT)},\tag{7}$$

where the elements $\langle\alpha_i|D_q^{(1)}|\beta_j\rangle$ are calculated according to Eq. (6). The preceding factor 1/2 takes into account that the population of each sublevel α_i is only 1/2 (since α is doubly degenerate). The last factor is the normalized occupation probability of the Stark level E_α in the ground state at thermal equilibrium. Each MD-generated configuration around a specific RE ion will correspond to a certain line with frequency $\nu_{\alpha\beta}=(E_\beta-E_\alpha)/h$ and oscillator strength $P_q(\alpha,\beta)$. Many configurations thus result in an normalized absorption band (histogram) $P_q^{\text{config}}(\alpha,\beta)$. It can be difficult or impossible to observe individual Stark-level contributions experimentally; the total contribution (for one RE ion) is then a summation of the Stark bands:

$$P_q^{\text{tot}}=\sum_{\alpha=1}^{J+1/2}\sum_{\beta=1}^{J'+1/2}P_q^{\text{config}}(\alpha,\beta).\tag{8}$$

Finally, the total spectral band are derived from this expression by also averaging the contributions from all RE ions in the MD simulation box. In this method, it is a simple matter to separate contributions originating from different sites. We have thus derived expressions for the polarized absorption

intensities for a RE ion in a material. The theory includes the orientations of the RE ions and the various energy splittings; the occupation probabilities are also different for the various ground-state Stark levels, depending on energy splitting and temperature. Also, by using a MD-based approach, dynamical properties and nonstoichiometry are taken into account.

Na^+/Nd^{3+} β''-ALUMINA HOST

The β''-aluminas are a family of solid-state ion (Na^+) conductors whose main applications lie in the area of advanced batteries. However, optical applications have also been speculated upon, since Na^+ ions can be exchanged for trivalent RE ions in the structure. Especially interesting is their potential use as optical amplifiers, which originates in the extremely high oscillator strength of the $^4G_{5/2}$ transition for Nd^{3+} exchange (an order of magnitude larger than in Nd:YAG). Lasing has been achieved in both pulsed- and continuous-wave modes.[28] The absorption spectrum for β''-alumina reflects its dual crystalline and liquidlike properties. The peaks are inhomogeneously broadened while, at low temperatures, it is still possible to resolve crystal-field splittings of individual multiplets from ions at distinctly different sites. The compound is nonstoichiometric, obtained by ion-exchange of the Na^+ ions for Nd^{3+} ions in Na^+ β''-alumina.[29] The layered structure consists of close-packed *spinel blocks* of Al^{3+}, Mg^{2+}, and O^{2-} interlayered by liquidlike *conduction planes* containing Na^+, Nd^{3+}, and supporting oxygen ions which bridge the spinel blocks through Al-O-Al bonds. Figure 1(a) is a schematic illustration of the block structure, while Fig. 1(b) illustrates the sites in the conduction plane. Two possible sites for the mobile cations are indicated in Fig. 1(b): the seven-coordinated Beevers-Ross (BR) site (C_{3v} symmetry) and the eight-coordinated mid-oxygen (MO) site (C_{2h} symmetry). In pure Na^+ β''-alumina, sodium ions occupy, on average, five out of six BR sites. X-ray diffraction studies carried out on 100% exchanged Nd^{3+} β''-alumina showed that 95% of the neodymium ions occupy MO sites.[30] In a mixed-ion Na^+/Nd^{3+} β''-alumina, where 64% of the sodium ions had been replaced by Nd^{3+} ions, approximately 2/3 of the neodymium ions were found at the MO sites.[19] Samples subjected to thermal treatment are known to behave differently, however. We focus here on Na^+/Nd^{3+} β''-alumina, where 20% of the sodium ions have been exchanged for Nd^{3+}. This low concentration corresponds to 12 Nd^{3+} ions in the chosen MD simulation box (four in each conduction plane). Several earlier experimental studies of various compositions of Na^+/Nd^{3+} β''-alumina[12,13,31] render this an ideal test of our method. We treat three specific energy levels: the ground level $^4I_{9/2}$, and the excited levels $^4F_{3/2}$ and $^2P_{1/2}$. The latter is particularly interesting since it remains a single level in a crystal field: a property which has been used experimentally to study different site occupations in Na^+/Nd^{3+} β''-alumina.[13,31,32]

CALCULATIONS

The dynamic and nonstoichiometric nature of the β''-alumina structure means that the environment around each Nd^{3+} ion is essentially unique, making it inappropriate to apply a crystal model based on ideal symmetry assumptions. Instead, we calculate the crystal-field parameters for each MD-generated Nd^{3+} environment. It is also important to take the correct average; it is clearly incorrect to average the atomic positions and form one environment and calculate the oscillator strength. Instead, the oscillator strength must be calculated for each possible environment, and an average then taken over the various oscillator strengths.

TABLE II. Values of MD potential parameters used in the simulation of Na^+/Nd^{3+} β''-alumina. Atom-pair combinations not listed are taken to be purely coloumbic, since they are well separated from one another, i.e., $A_{ij}=C_{ij}=0$.

i	j	A_{ij} (eV)	ρ_{ij} (Å)	C_{ij} (eV Å^6)
Al	O	1 460.3	0.299 12	0
Al	Na	15 240.0	0.146 20	0
O	O	22 764.3	0.149	27.8
O	Mg	1 428.5	0.294 5	0
O	Na	1 126.8	0.306 5	0
O	Nd	1 100.0	0.37	0
Na	Na	9 597.4	0.167 89	0
Na	Nd	15 240.0	0.146 20	0

The molecular-dynamics technique used has been described in detail elsewhere.[11,33–35] The standard ion pair potentials are of the Born-Mayer-Huggins form $[V_i=\Sigma_{i\neq j}q_iq_j/r_{ij}+A_{ij}\exp(-r_{ij}/\rho_{ij})-C_{ij}/r_{ij}^6]$; the parameters used are listed in Table II (see Refs. 36 and 37). The simulations were performed for a Na^+/Nd^{3+} β''-alumina composition corresponding to 20% of the sodium ions exchanged for Nd^{3+}. The $6a\times6b\times1c$ simulation box, containing 3180 ions, was initialized and equilibrated at 1000 K for 4000 time steps, each of 2.0 fs. Thereafter, the temperature was lowered stepwise to 300 K and 9 K, respectively, and further equilibration made for at least 1000 steps at each temperature. The positions of all ions in the simulation box were then stored for every fourth time step during the two sampling runs, each of 800 steps. The $A_{t,p}$ parameters [Eq. (1)] were then calculated using these configurations for each of the 12 Nd^{3+} ions in the simulation box. The crystal field experienced by a Nd^{3+} ion is calculated by a direct summation of all ligands within a 25-Å sphere around the ion. This gave complete convergence for the relevant ($t\neq1$) CFP's. The CFP's obtained were then used to calculate the elements in the energy matrix [Eqs. (2) and (3)], which was then diagonalized to obtain the eigenvalues and eigenfunctions for each MD-generated configuration. The intensities were then calculated according to Eqs. (7) and (8). The number of Nd^{3+} ions in the simulation box (12) and the number of configurations stored (200) means that 200×12 environments are used in the calculation. Further improvement of the statistics is needed, however, especially for low temperatures. In the laser absorption experiments of Dai *et al.*,[13] the incident radiation field vectors $\mathbf{E}\perp\mathbf{c}$ and $\mathbf{E}\|\mathbf{c}$ correspond to σ and π polarization, respectively. In Eqs. (7) and (8), the polarized oscillator strengths are calculated according to $P_\sigma=(P_1+P_{-1})/2$ and $P_\pi=P_0$. Three different levels were chosen for this study: the ground state $^4I_{9/2}$, and the two excited states, $^4F_{3/2}$ and $^2P_{1/2}$. In this work, we neglect J-J mixing as well as intermediate coupling effects. They are

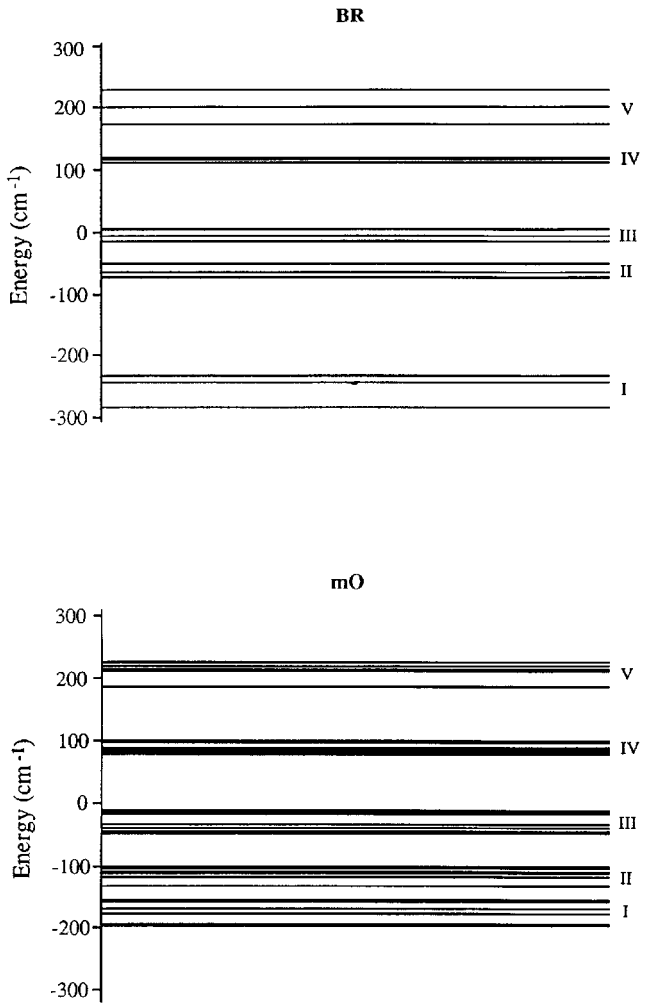

FIG. 2. Ground-state Stark splitting ($^4I_{9/2}$) for the BR and MO sites, averaged over 200 MD-generated configurations obtained at 9 K.

known to be small for these states,[4,5] so that RS coupling is a good approximation. Neither is configuration interaction included since these energy levels lie low in energy. The calculation of oscillator strengths for these two transitions are facilitated by the fact that $\langle i\|U^{(2)}\|f\rangle$ is zero. Hence, A_{1p}, which converges very slowly because of its R^{-2} dependence [see Eq. (1)], is not included. The shielding parameters were taken from Ref. 8. In the spectra presented below, the Stark-energies are given relative to the energy for the unperturbed state, the so-called ''free-ion'' levels. These were calculated by Rajnak[5] for Nd^{3+}.

RESULTS AND DISCUSSION

The MD simulations of Na^+/Nd^{3+} β''-alumina resulted in three Nd^{3+} ions at BR sites and nine at MO sites at both 9 and 300 K. Different initializing schemes were investigated, but these resulted only in small variations in ordering within the conduction planes. To our knowledge, no corresponding diffraction study has been made for this 20% Nd^{3+} substituted composition.

The $^4I_{9/2}$ ground-state splitting can be studied directly using the present technique. Figure 2 shows the average energies for the ions at the MO and BR sites, respectively, for the 9-K simulation. The two sites result in two distinctly different energy distributions. The overall splitting for the BR site is $\sim$500 cm^{-1}, and $\sim$400 cm^{-1} for the MO site. The splittings within the multiplets are also distributed differently. We can note that the experimental ground-state splitting in Na^+/Er^{3+} β''-alumina is $\sim$550 cm^{-1} for the Er^{3+} ions at BR sites,[38] and $\sim$500 and 560 cm^{-1}, respectively, for Er^{3+} and Nd^{3+} ions in the Y_2O_3 host.[6] This suggests that the splittings calculated here are slightly too small. The most probable reasons for this are (i) inaccuracy in the shielding parameters, especially for σ_2, which has the largest effect on the energies (changing σ_2 from 0.792 to 0.7 causes an increase in the overall splitting of 50–60 cm^{-1}); and (ii) uncertainty in the radial integrals, of which $\langle r^6\rangle$ is the most sensitive,[9] since it has such high power. Increasing this parameter by 25% again leads to an increase in the splitting of the same magnitude as (i). The choice of potential parameters and the validity of a point-charge crystal-field model also influence the energy eigenvalues slightly. An interesting observation is that the energy difference between the first and second Stark level is much higher for BR than MO sites. Experimentally, Dunn *et al.*[31] observed that the temperature dependence of the transition $^2P_{1/2}$ is small, and suggested that the first Stark level of $^4I_{9/2}$ is widely separated from the next. This is consistent with our calculation if BR occupation dominates in their sample. It should be noted, however, that the temperature dependence of a transition is also related to the polarization of the incoming light; σ-polarized light was used in their experiment.

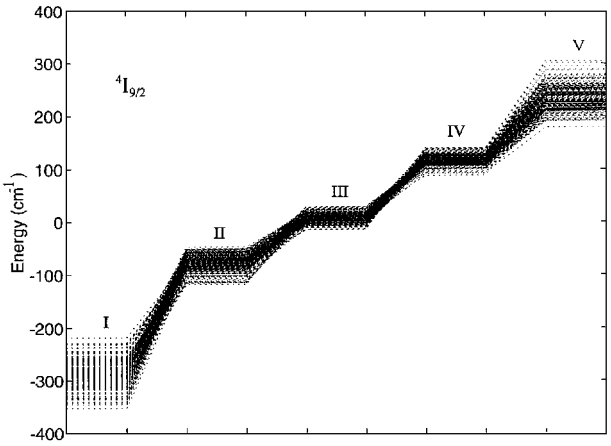

FIG. 3. Instantaneous Stark energies ($^4I_{9/2}$) at each of the 200 MD-generated configurations for an ion occupying a BR site at 300 K.

The sensitivity of the five ground-state Stark levels is shown in Fig. 3. The figure shows the instantaneous splitting for each MD-generated configuration around one Nd^{3+} ion at a BR site at 300 K. The levels furthest away from the baricenter of the multiplet are the most sensitive.

Figure 4 shows the energy splitting of the $^4F_{3/2}$ level for the MO and BR sites at 9 K. The calculated energies and splittings agree quite well with experiment. The energy splitting for BR sites ($\sim$210 cm^{-1}) is greater than for MO sites ($\sim$140 cm^{-1}). The experimental values for a 38.5% exchanged sample are $\sim$200 and $\sim$160 cm^{-1}, respectively.[13]

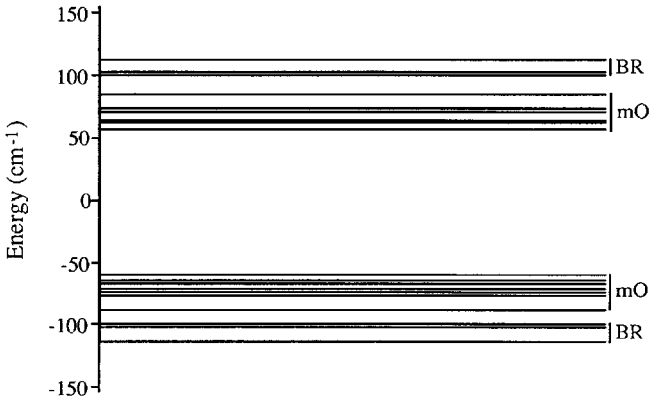

FIG. 4. Stark splitting of the $^4F_{3/2}$ level for the 12 Nd^{3+} ions in the simulation box (3 BR and 9 MO) averaged over 200 configurations.

According to Kramer's theorem, the $^2P_{1/2}$ level is not split for one specific site ($J+1/2=1$); the observed splitting could then be due to the occupation of two distinct sites (MO and BR). However, in the 2×2 Hermitian matrix for the $^2P_{1/2}$ level, the off-diagonal elements are zero, and summation of the diagonal elements yields a negligible contribution. The single level of this state remains essentially unchanged when the ion is placed in a crystal field, i.e., the $^2P_{1/2}$ Stark level has the same energy for both BR and MO sites. The observed separation must therefore be a result of the lowest Stark level of the ground state having different energies for the two sites. This energy difference is $\sim100\ cm^{-1}$ (see Fig. 2), and is quite close to the experimental value ($\sim120\ cm^{-1}$ between the peaks), see Fig. 5 in Ref. 13.

The method used for calculating oscillator strength has been refined [Eqs. (7) and (8)]; the theory takes into account both the polarization of the incoming light and the orientation of the RE ion for a certain environment. The $^4I_{9/2}\rightarrow{}^2P_{1/2}$ transition at 9 K is shown in Fig. 5(a) for both σ and π polarization. Although our calculations (for a 20% exchanged sample) cannot be compared directly with the experimental polarized absorption study (38.5% exchanged),[13] some general observations can be made. Our calculation [Fig. 5(a)] shows clearly that σ polarization dominates around 428–429 nm (BR sites), and that σ and π polarization are roughly equal (unpolarized) around 430–431 nm (MO); this agrees with Fig. 5 of Ref. 13. However, our calculation shows the intensity at 428–429 nm to be smaller than the intensity at 430–431 nm, while the reverse is observed in Ref. 13. To bring our calculated spectrum into better agreement with experiment, we would need a higher Nd^{3+} occupation near BR sites. Further, our calculation for the $^4I_{9/2}\rightarrow{}^4F_{3/2}$ transition at 9 K [Fig. 5(b)] can be compared with Fig. 6 in Ref. 13. We see that π polarization dominates around 855–865 nm (BR), whereas σ polarization dominates at 870–880 nm (BR and MO); again in qualitative agreement with Ref. 13. Finally, a rather large intensity is calculated at $\sim$870 nm, which is totally missing from the experimental result. Fig. 5(c) shows the intensity from ions in BR sites only; the peak slightly below 870 nm has now disappeared, and the overall agreement with the experimental spectrum is now much better. Higher BR site occupation is again seen to be the key to achieving better agreement.

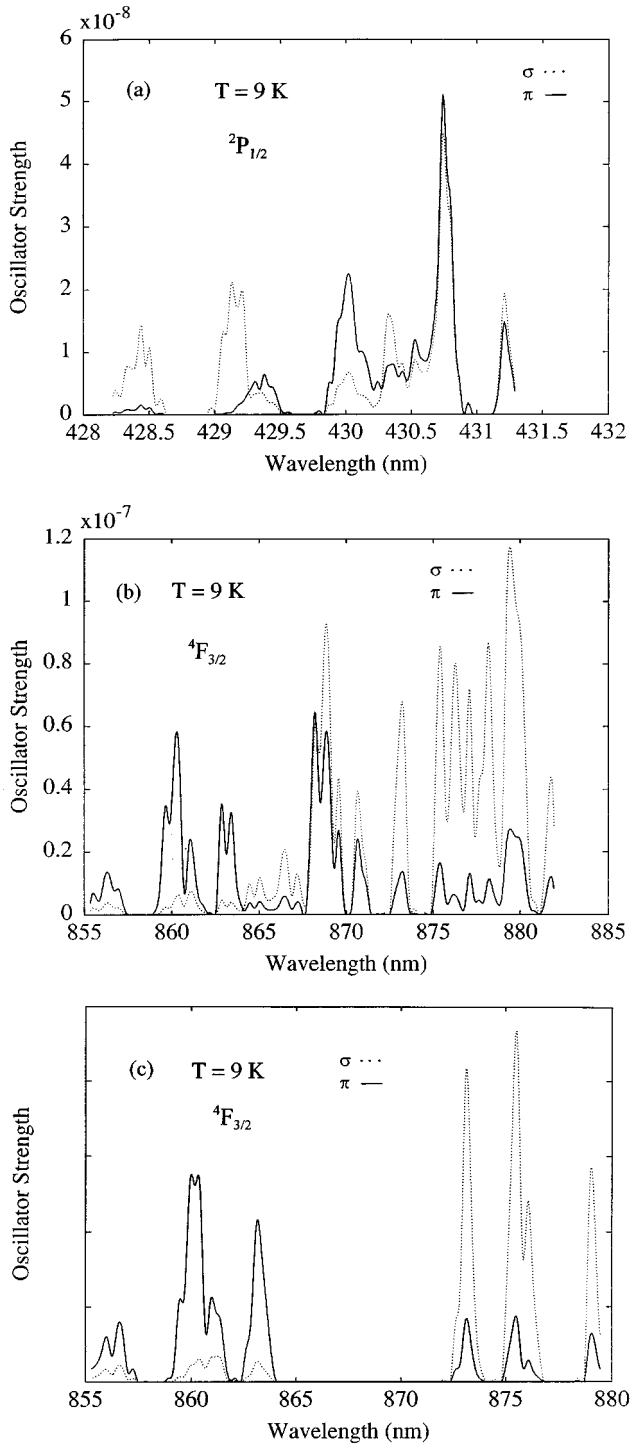

FIG. 5. The calculated polarized absorption spectrum averaged over 200 configurations, as obtained from a MD simulation at 9 K. All transitions originate from the lowest Stark level in the ground state $^4I_{9/2}$; (a) The $^2P_{1/2}$ transition, where the BR and MO contributions are found at 428–429.5 nm and 430–431.5 nm, respectively. (b) The $^4F_{3/2}$ transition. The BR contributions are found at 855–865 nm (upper Stark level) and 872–880 nm (lower); the MO contributions are at 865–871 nm (upper) and 875–881 nm (lower). (c) The $^4F_{3/2}$ transition originating from BR sites alone. The curves are fitted to a histogram (resolution: 100 intervals for each band) using cubic spline interpolation.

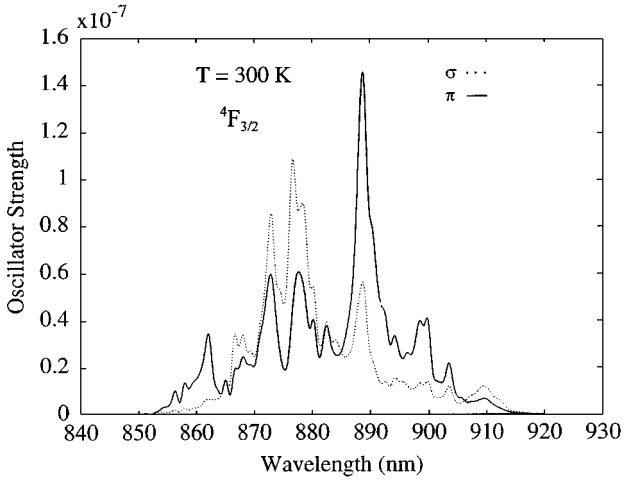

FIG. 6. The $^4F_{3/2}$ transition at 300 K averaged over 200 configurations.

The BR MO occupation ratio is known from x-ray diffraction studies of a 100% exchanged sample to be ca. 5%/95%.[30] A 35%/65% ratio is obtained for a 64% exchanged sample in another diffraction study,[19] where it was speculated that the presence of Na^+ ions, which occupy BR sites in the Na^+ β''-alumina structure, caused some Nd^{3+} ions to leave their MO sites. It is most likely that BR site occupation will be even higher in the 20% exchanged sample, bringing our calculated intensities into quantitative agreement with experiment. Heat treatment is also known to influence the absorption spectrum.[32] For example, the $^2P_{1/2}$ transition for a 60%-exchanged sample shows equal intensities at 428 and 430 nm for a ''slow cooled'' sample (held at $T\sim600$ K for several days), while the peak at 428 nm (BR) becomes stronger and at 430 nm (MO) weaker for a ''quenched'' (normal cooling) sample, implying a higher BR occupation. High-resolution transmission electron microscopy (HRTEM) studies of both fully and partially exchanged systems suggest ordering of the Nd^{3+} ions after annealing, to give extended —Nd—O—Nd—O—Nd— chains in the conduction plane. However, this ordering was not maintained at low Nd^{3+} concentrations.[39] Three factors thus combine to suggest that the relative BR site occupation was high in the sample used in Ref. 13: no heat treatment, low Nd^{3+} concentration, and our optical calculations.

Further, the optical absorption spectrum for Na^+/Nd^{3+} β''-alumina at higher temperatures contains contributions from ions with a wide variety of environments, leading to inhomogeneously broadened lines. There is also a contribution from temperature broadening, with contributions coming from all Stark levels in the ground state. Figure 6 is similar to Fig. 5(b), except that the calculation is now made at room temperature. Our calculation of the $^4I_{9/2}\rightarrow{}^4F_{3/2}$ transition at 300 K (Fig. 6) shows that the π-polarized spectrum dominates at the edges of the spectral line, whereas the σ-polarized spectrum dominates at the center. This agrees with Fig. 3 in Ref. 13, but the π-polarized intensity at $\sim$860 nm is again too low compared with experiment, and too high at $\sim$870 nm. We know from the low-temperature results [Figs. 5(b) and 5(c)] that the intensities at 860 and 870 nm originate from BR and MO site occupation, respectively. The

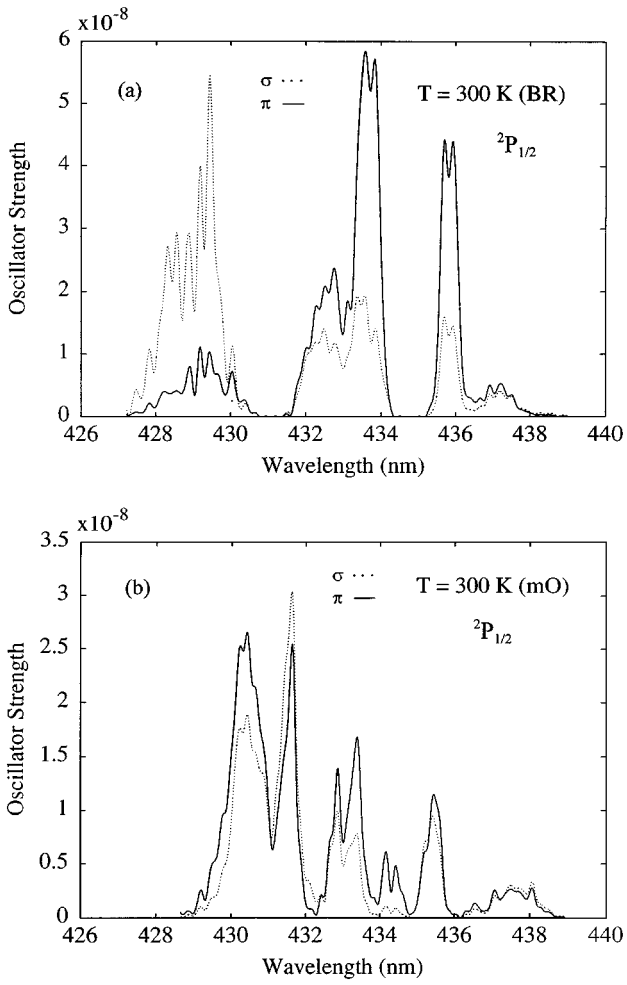

FIG. 7. The polarized $^2P_{1/2}$ transition at 300 K where the BR (a) and MO (b) contributions have been separated.

general observation from Fig. 6 is that, also at room temperature, higher BR and lower MO occupation is needed to achieve better agreement with experiment. The strong σ-polarized peak at 872–880 nm originates from both BR and MO sites. Peaks above 880 nm result from the occupation of the higher Stark levels in the ground state. The total broadening of these calculated room-temperature spectra seems to agree well with experiment, although it is interesting to note that experimental results at 573 K (Fig. 4 in Ref. 13) agree much better with our Fig. 6, most likely indicating higher MO site occupancy at higher temperature (remembering the 9/12 MO fraction from our MD simulation). This is consistent with the above discussion relating to heat treatment: higher MO occupancy is expected for heat-treated samples.[32] The extreme cases of full BR (a) and MO (b) occupation are plotted separately for the $^2P_{1/2}$ transition at $T=300$ K (Fig. 7).

Dai *et al.*[13] have integrated their experimental spectra to obtain the oscillator strengths for both polarizations; these are compared with our calculated values in Table III. It is of interest to make a rough assessment as to whether agreement with experiment (Table III) can be improved using Ref. 12, where the Nd^{3+} concentration dependence of the $\Omega_{\lambda\sigma}$ parameters are plotted (their Fig. 4). The spectra in Ref. 12 were measured at room temperature for the σ-polarization case

TABLE III. Integrated polarized oscillator strengths at 300 K from a simulation of 20% exchanged Na^+/Nd^{3+} β''-alumina and experimental values for a 38% exchanged sample (Ref. 13). Experimental values (20%) using Fig. 4 in Ref. 12 are also given. All oscillator strengths are in units of 10^{-6}.

	Theory (20%) 300 K			Expt. (38%) 300 K		Expt. (20%) 300 K
Transition	P_σ	P_π	$P_{\text{unpol.}}$	P_σ	P_π	P_σ
$^4I_{9/2}\rightarrow{}^4F_{3/2}$	2.0	2.38	2.13	1.34	1.91	2.3
$^4I_{9.2}\rightarrow{}^2P_{1/2}$	0.54	0.64	0.57	0.29	0.27	0.58

only. Our calculations (for 20% exchange) correspond to 3.6×10^{20} ions/cm^3. We see that going from 7×10^{20} to 3.6×10^{20} ions/cm^3 causes an increase in $\Omega_{4\sigma}$ by a factor 2.0. This is precisely what is needed to bring our $^2P_{1/2}$ results into quantitative agreement with experiment (see last column in Table III). The $^4F_{3/2}$ transition depends on Ω_4 and Ω_6; lowering the concentration increases $\Omega_{4\sigma}$ and $\Omega_{6\sigma}$ by a factor 2.0 and 1.7, respectively, bringing also the $^4F_{3/2}$ results for σ polarization into quantitative agreement with experiment. Oscillator strength can be related crudely to site occupation in the following way: $P_q=\rho_{\text{BR}}\langle P_{q(\text{BR})}\rangle+\rho_{\text{MO}}\langle P_{q(\text{MO})}\rangle$, where ρ_{site} is the fraction and $\langle P_{q(\text{site})}\rangle$ is the average oscillator strength for a particular site. We find, for the $^4F_{3/2}$ transition at 300 K, that the calculated averages are (in 10^{-6}): $\langle P_{\sigma(\text{BR})}\rangle=2.4$, $\langle P_{\sigma(\text{MO})}\rangle=1.9$, $\langle P_{\pi(\text{BR})}\rangle=3.7$, and $\langle P_{\pi(\text{MO})}\rangle=2.0$. From our simulation ρ_{BR} and ρ_{MO} are 3/12 and 9/12, respectively. For a 20% exchanged sample, this gives $2.0\times10^{-6}<P_\pi<3.7\times10^{-6}$ and $1.9\times10^{-6}<P^\sigma\leqslant2.4\times10^{-6}$. Using the experimental value $P_\sigma=2.3\times10^{-6}$ from the last column of Table II gives $\rho_{\text{BR}}=0.8$. Similarly, the $^2P_{1/2}$ transition at 300 K gives $5.7\times10^{-7}<P_\pi<7.5\times10^{-7}$ and $4.6\times10^{-7}<P_\sigma<6.7\times10^{-7}$, so that $\rho_{\text{BR}}=0.57$. Accumulated evidence would thus suggest that the fraction of Nd^{3+} ions in BR sites is in excess of 50% in their 20% exchanged sample.[12]

We can note, however, that the deduced BR fraction (>50% for samples with low Nd^{3+} concentration) does not correspond to the MD-generated fraction (3/12). This is not surprising, since the samples in Refs. 12 and 13 were not heat treated. An equilibrated sample would clearly result in a fraction closer to that obtained from our MD simulation.

CONCLUSIONS

A MD-based approach is clearly essential in the treatment of complex materials in that MD takes account of a whole range of possible environments around the RE ions. Moreover, complications relating to nonstoichiometry and artificially imposed symmetry are removed. It is demonstrated that our general approach works well; the features in the theoretical spectra correspond satisfactorily with experiment at different temperatures. Especially noteworthy is that the trends in the experimental polarized spectra can be reproduced. The method can also be applied to complex amorphous materials, e.g., glasses, polymers, and liquids, provided that a more sophisticated ligand-field model is used to take into account polarizability and covalency effects.

ACKNOWLEDGMENTS

This work has been supported in part by the United States Office of Naval Research (ONR) and in part by the Swedish Natural Science Research Council (NFR).

[1] B. R. Judd, Phys. Rev. **127**, 750 (1962).
[2] G. S. Ofelt, J. Chem. Phys. **37**, 511 (1962).
[3] B. G. Wybourne, J. Chem. Phys. **32**, 639 (1960).
[4] B. G. Wybourne, J. Chem. Phys. **34**, 279 (1961).
[5] K. Rajnak, J. Chem. Phys. **43**, 847 (1965).
[6] W. F. Krupke, Phys. Rev. **145**, 325 (1966).
[7] R. M. Sternheimer, M. Blume, and R. F. Peierls, Phys. Rev. **173**, 376 (1968).
[8] D. Sengupta and J. O. Artman, Phys. Rev. B **1**, 2986 (1970).
[9] G. Burns, J. Chem. Phys. **42**, 377 (1965).
[10] S. Edvardsson, M. Wolf, and J. O. Thomas, Phys. Rev. B **45**, 10 918 (1992).
[11] M. Wolf, S. Edvardsson, M. A. Zendejas, and J. O. Thomas, Phys. Rev. B **48**, 10 129 (1993).
[12] A. J. Alfrey, O. M. Stafsudd, B. Dunn, and D. L. Yang, J. Chem. Phys. **88**, 707 (1988).
[13] H. Dai and O. M. Stafsudd, J. Phys. Chem. Solids **52**, 367 (1991).
[14] C. Göller-Walrand, D. Fluyt, P. Porcher, A. A. S. Da Gama, G. F. de Sa, W. T. Carnall, and G. L. Goodman, J. Less-Common Met. **148**, 339 (1989).
[15] M. Faucher and D. Garcia, Phys. Rev. B **26**, 5451 (1982).
[16] M. J. Weber and S. A. Brawer, J. Non-Cryst. Solids **52**, 321 (1982).
[17] D. J. Newman, Adv. Phys. **20**, 197 (1971).
[18] C. A. Morrison and R. P. Leavitt, in *Handbook of the Physics and Chemistry of Rare Earths*, edited by K. A. Gschneider, Jr. and L. Eyring (North-Holland, Amsterdam, 1982), Vol. 5, p. 486.
[19] M. Wolf and J. O. Thomas, Acta Cryst. B **49**, 491 (1993).
[20] M. A. Salzberg and G. C. Farrington, J. Solid State Chem. **83**, 272 (1989).
[21] M. Wolf and J. O. Thomas, J. Mater. Chem. **4**, 839 (1994).
[22] M. L. den Boer, Y. S. Pak, K. J. Adamic, S. G. Greenbaum, M. C. Wintersgill, J. F. Lomax, J. J. Fontanella, B. Dunn, and G. C. Farrington, Phys. Rev. B **45**, 6369 (1992).
[23] K. W. H. Stevens, Proc. Phys. Soc. London, A **65**, 209 (1952).
[24] B. R. Judd, *Operator Techniques in Atomic Spectroscopy*

(McGraw-Hill, New York, 1963).
[25] E. Condon and G. Shortley, *The Theory of Atomic Spectra* (Cambridge University Press, Cambridge, 1951).
[26] G. Racah, Phys. Rev. **76**, 1352 (1949).
[27] E. Merzbacher, *Quantum Mechanics*, 2nd ed. (Wiley, New York, 1970), pp. 406–408.
[28] M. Jansen, A. J. Alfrey, O. M. Stafsudd, D. L. Yang, B. Dunn, and G. C. Farrington, Opt. Lett. **9**, 119 (1984).
[29] B. Dunn and G. C. Farrington, Solid State Ion. **9-10**, 223 (1983).
[30] W. Carrillo-Cabrera, J. O. Thomas, and G. F. Farrington, Solid State Ion. **28-30**, 317 (1988).
[31] B. Dunn, D. L. Yang, and D. Vivien, J. Solid State Chem. **73**, 235 (1988).
[32] R. B. Queenan and P. K. Davis, Solid State Ion. **28-30**, 358 (1988).
[33] S. Edvardsson and J. O. Thomas, J. Phys. Condens. Matter **6**, 1319 (1994).
[34] M. A. Zendejas and J. O. Thomas, Phys. Scr. **47**, 440 (1993).
[35] W. Smith and M. J. Gillan, J. Phys. Condens. Matter **4**, 3215 (1992).
[36] G. V. Lewis and C. R. A. Catlow, J. Phys. C **18**, 1149 (1985).
[37] J. R. Walker and C. R. A. Catlow, J. Phys. C **15**, 6151 (1982).
[38] H. Dai, Ph.D. thesis, University of California, Los Angeles, 1990 (unpublished).
[39] P. Davies, A. Petford and M. O'Keefe, Solid State Ion. **18-19**, 624 (1986).
[40] K. L. Van der Sluis and L. J. Nugent, J. Chem. Phys. **60**, 1927 (1974).